



# Synthesis, structural characterization and optical properties of a new cesium aluminum borate, $\text{Cs}_2\text{Al}_2\text{B}_2\text{O}_7$

Kai Feng<sup>a,b,c</sup>, Wenlong Yin<sup>a,b,c</sup>, Jiyong Yao<sup>a,b,\*</sup>, Yicheng Wu<sup>a,b</sup>

<sup>a</sup> Center for Crystal Research and Development, Technical Institute of Physics and Chemistry, Chinese Academy of Sciences, Beijing 100190, PR China

<sup>b</sup> Key Laboratory of Functional Crystals and Laser Technology, Technical Institute of Physics and Chemistry, Chinese Academy of Sciences, Beijing 100190, PR China

<sup>c</sup> Graduate University of the Chinese Academy of Sciences, Beijing 100049, PR China

## ARTICLE INFO

### Article history:

Received 1 September 2011

Received in revised form

12 October 2011

Accepted 14 October 2011

Available online 25 October 2011

### Keywords:

$\text{Cs}_2\text{Al}_2\text{B}_2\text{O}_7$

Synthesis

Crystal structure

Optical property

## ABSTRACT

A new borate,  $\text{Cs}_2\text{Al}_2\text{B}_2\text{O}_7$ , was synthesized by solid-state reaction. It crystallizes in the monoclinic space group  $P2_1/c$  with  $a=6.719(1)$  Å,  $b=7.121(1)$  Å,  $c=9.626(3)$  Å,  $\beta=115.3(1)^\circ$ , and  $Z=2$ . In the structure, two  $\text{AlO}_4$  tetrahedra and two  $\text{BO}_3$  planar triangles are connected alternately by corner-sharing to form nearly planar  $[\text{Al}_2\text{B}_2\text{O}_{10}]$  rings, which are further linked via common O1 atom to generate layers in the  $bc$  plane. These layers then share the O3 atoms lying on a center of inversion to form a three-dimensional framework with Cs atoms residing in the channels. The IR spectrum confirms the presence of both  $\text{BO}_3$  and  $\text{AlO}_4$  groups and the UV–vis–IR diffuse reflectance spectrum indicates a band gap of about 4.13(2) eV.

© 2011 Elsevier Inc. All rights reserved.

## 1. Introduction

Research on borate compounds has long time been stimulated by their rich structural chemistry and interesting physical properties [1–9]. Boron atoms usually adopt triangular or tetrahedral oxygen coordination to form  $\text{BO}_3$  or  $\text{BO}_4$  groups, which can be linked further to form linear, layered and three-dimensional structures. For compounds with the  $M_2\text{Al}_2\text{B}_2\text{O}_7$  ( $M$ =alkali metal) composition, known members include  $\text{Na}_2\text{Al}_2\text{B}_2\text{O}_7$ ,  $\text{K}_2\text{Al}_2\text{B}_2\text{O}_7$ , and  $\text{Rb}_2\text{Al}_2\text{B}_2\text{O}_7$ . With the increase of alkali metal ionic radius, the structure of  $M_2\text{Al}_2\text{B}_2\text{O}_7$  changes from trigonal system ( $\text{Na}_2\text{Al}_2\text{B}_2\text{O}_7$  ( $P\bar{3}1c$ ) and  $\text{K}_2\text{Al}_2\text{B}_2\text{O}_7$  ( $P321$ )) to monoclinic system ( $\text{Rb}_2\text{Al}_2\text{B}_2\text{O}_7$  ( $P2_1/c$ )) [10–12]. Among them,  $\text{K}_2\text{Al}_2\text{B}_2\text{O}_7$  adopts a non-centrosymmetric structure and exhibits good nonlinear optical (NLO) properties [10], while the other two are centrosymmetric without NLO effect. The diverse structural types in this series of compounds inspire us to further investigate the  $M_2\text{Al}_2\text{B}_2\text{O}_7$  ( $M$ =alkali metal) compounds with emphasis on the largest alkali metal Cs and smallest alkali metal Li. The preparation of  $\text{Li}_2\text{Al}_2\text{B}_2\text{O}_7$  is unsuccessful; however, the  $\text{Cs}_2\text{Al}_2\text{B}_2\text{O}_7$  compound has been synthesized successfully. Interestingly, it crystallizes in a different structure from the three known  $M_2\text{Al}_2\text{B}_2\text{O}_7$  ( $M$ =Na, K, Rb) borates, which further demonstrates the

influence of ionic radius on structure transformation. In this paper, we report the crystal growth, structure, and optical property of  $\text{Cs}_2\text{Al}_2\text{B}_2\text{O}_7$ .

## 2. Experimental

### 2.1. Solid-state synthesis

$\text{Cs}_2\text{Al}_2\text{B}_2\text{O}_7$  is a new phase found in the  $\text{Cs}_2\text{O}-\text{Al}_2\text{O}_3-\text{B}_2\text{O}_3$  system. The sample was synthesized via solid-state reaction using a mixture of  $\text{Cs}_2\text{CO}_3$  (AR),  $\text{Al}_2\text{O}_3$  (AR) and  $\text{H}_3\text{BO}_3$  (AR) that was heated progressively up to 1000 °C. Polycrystalline sample corresponding to the  $\text{Cs}_2\text{CO}_3:\text{Al}_2\text{O}_3:3\text{H}_3\text{BO}_3$  molar ratio produced a single-phase product. X-ray powder diffraction analysis of the resultant powder sample was performed at room temperature in the angular range of  $2\theta=10-70^\circ$  with a scan step width of  $0.02^\circ$  and a fixed counting time of 1 s/step using an automated Bruker D8 X-ray diffractometer equipped with a diffracted monochromator set for  $\text{Cu } K\alpha$  ( $\lambda=1.5418$  Å) radiation. It did not resemble any pattern in the database and was later found to be in excellent agreement with the calculated pattern on the basis of the single crystal crystallographic data of  $\text{Cs}_2\text{Al}_2\text{B}_2\text{O}_7$  (Fig. 1).

### 2.2. Single-crystal growth

A mixture of the as-synthesized  $\text{Cs}_2\text{Al}_2\text{B}_2\text{O}_7$  powder, LiF and KF (acting as flux to lower the melting point) in molar ratio of 1:1:1

\* Corresponding author at: Center for Crystal Research and Development, Technical Institute of Physics and Chemistry, Chinese Academy of Sciences, Beijing 100190, PR China. Fax: +86 10 82543725.

E-mail address: [jjyao@mail.ipc.ac.cn](mailto:jjyao@mail.ipc.ac.cn) (J. Yao).

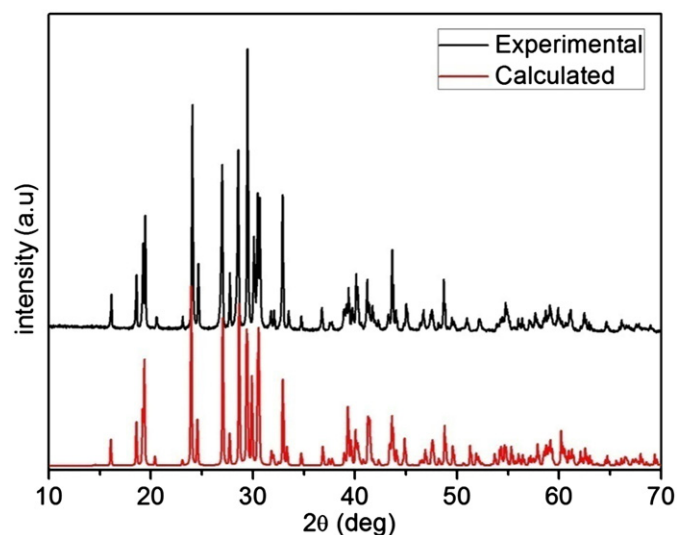


Fig. 1. Experimental (top) and calculated (bottom) x-ray powder diffraction data of  $\text{Cs}_2\text{Al}_2\text{B}_2\text{O}_7$ .

was ground in an agate mortar and loaded into a platinum crucible. The sample was placed in a computer-controlled furnace, heated to 900 °C in 15 h and kept there for 24 h, then cooled at a slow rate of 3 °C/h to 600 °C, and finally cooled to room temperature. The product consisted of colorless block crystals, which were manually selected for structure characterization. Analysis of the crystals with an EDX-equipped Hitachi S-3500 SEM showed the presence of Cs and Al in the approximate molar ratio of 1:1.

### 2.3. Structure determination

Single-crystal X-ray diffraction data were collected with the use of graphite-monochromatized Mo  $K\alpha$  ( $\lambda=0.71073$  Å) at 93 K on a Rigaku AFC10 diffractometer equipped with a Saturn CCD detector. Crystal decay was monitored by re-collecting 50 initial frames at the end of data collection. The collection of the intensity data was carried out with the program Crystalclear [13]. Cell refinement and data reduction were carried out with the use of the program Crystalclear [13], and face-indexed absorption corrections were performed numerically with the use of the program XPREP [14].

The structure was solved with the direct methods program SHELXS and refined with the least-squares program SHELXL of the SHELXTLPC suite of programs. The final refinement included anisotropic displacement parameters and a secondary extinction correction. The program STRUCTURE TIDY [15] was then employed to standardize the atomic coordinates. Additional experimental details are given in Table 1. The final refined atomic positions and isotropic thermal parameters are summarized in Table 2 and selected metrical data are given in Table 3. Further information can be found in Supplementary Material.

### 2.4. Infrared spectroscopy

Infrared spectrum was recorded on Shimadzu IR Affinity-1 Fourier transform infrared spectrometer in the 400–3000  $\text{cm}^{-1}$  range. The sample was mixed thoroughly with dried KBr (5 mg sample and 500 mg KBr).

### 2.5. Diffuse reflectance spectroscopy

A Cary 5000 UV–visible–NIR spectrophotometer with a diffuse reflectance accessory was used to measure the spectrum of  $\text{Cs}_2\text{Al}_2\text{B}_2\text{O}_7$  over the range 200 nm (6.20 eV) to 2500 nm (0.50 eV).

Table 1  
Crystal data and structure refinements for  $\text{Cs}_2\text{Al}_2\text{B}_2\text{O}_7$ .

	$\text{Cs}_2\text{Al}_2\text{B}_2\text{O}_7$
fw	453.40
$a$ (Å)	6.719(1)
$b$ (Å)	7.121(1)
$c$ (Å)	9.626(3)
$\beta$	115.25(2)
Space group	$P2_1/c$
$V$ (Å <sup>3</sup> )	416.5(2)
$Z$	2
$T$ (K)	93(2)
$\lambda$ (Å)	0.71073
$\rho_c$ (g/cm <sup>3</sup> )	3.615
$\mu$ (cm <sup>-1</sup> )	8.960
$R1^a$	0.0232
$wR2^b$	0.0547

$$^a R1 = \sum ||F_o| - |F_c|| / \sum |F_o| \text{ for } F_o^2 > 2\sigma(F_o^2).$$

$$^b wR2 = \{ \sum [w(F_o^2 - F_c^2)]^2 / \sum wF_o^4 \}^{1/2} \text{ for all data. } w^{-1} = \sigma^2(F_o^2) + (zP)^2, \text{ where } P = (\text{Max}(F_o^2, 0) + 2 F_c^2) / 3; z = 0.02.$$

Table 2

Atomic coordinates and equivalent isotropic displacement parameters (Å) for  $\text{Cs}_2\text{Al}_2\text{B}_2\text{O}_7$ .

Atom	x	y	z	$U_{eq}^a$
Cs	0.77579(3)	0.36260(3)	0.11671(2)	0.01041(10)
Al	0.23909(17)	0.11880(14)	0.03980(12)	0.0055(2)
B	0.3534(6)	0.3893(5)	0.2752(4)	0.0070(7)
O1	0.2542(4)	0.3402(3)	0.1225(3)	0.0099(5)
O2	0.2595(4)	0.3313(4)	0.3691(3)	0.0146(6)
O3	0	0	0	0.0209(9)
O4	0.5390(5)	0.4942(5)	0.3274(3)	0.0224(7)

<sup>a</sup>  $U_{eq}$  is defined as one third of the trace of the orthogonalized  $U_{ij}$  tensor.

Table 3

Selected bond lengths (Å) and bond angles (deg.) for  $\text{Cs}_2\text{Al}_2\text{B}_2\text{O}_7$ .

Cs–O1	3.070(3)	Cs–O4	3.552(3)
Cs–O1	3.195(3)	Cs–O4	3.600(3)
Cs–O1	3.532(3)	Al–O1	1.749(3)
Cs–O2	3.127(3)	Al–O2	1.743(3)
Cs–O2	3.353(3)	Al–O3	1.708(1)
Cs–O2	3.545(3)	Al–O4	1.738(3)
Cs–O3	3.4120(5)	B–O1	1.375(4)
Cs–O3	3.478(1)	B–O2	1.368(4)
Cs–O4	3.205(3)	B–O4	1.353(4)
O3–Al–O4	110.0(1)	O3–Al–O1	114.5(1)
O3–Al–O2	109.5(1)	O2–B–O1	118.7(3)
O4–Al–O1	105.1(1)	O4–B–O2	122.2(3)
O2–Al–O1	103.5(1)	O4–B–O1	119.1(3)
O4–Al–O2	114.2(1)	Al–O3–Al	180.0(1)

## 3. Results and discussion

### 3.1. Solid-state synthesis and crystal growth

The presence of Cs makes the powder absorb moisture easily. By repeated grinding and sintering, and gradually elevating the sintering temperature from 200 to 1000 °C, we finally obtained pure  $\text{Cs}_2\text{Al}_2\text{B}_2\text{O}_7$  sample, as indicated in Fig. 1.

Owing to the high melting point of  $\text{Cs}_2\text{Al}_2\text{B}_2\text{O}_7$ , KF and LiF were used as flux to grow  $\text{Cs}_2\text{Al}_2\text{B}_2\text{O}_7$  crystal. Colorless and transparent block crystals with sizes up to  $2 \times 1 \times 1$  mm<sup>3</sup> were isolated, which were used in single-crystal X-ray diffraction data collection.

### 3.2. Structure

$\text{Cs}_2\text{Al}_2\text{B}_2\text{O}_7$  crystallizes in a new structure type in the centrosymmetric space group  $P2_1/c$  of the monoclinic system with  $a=6.719(1)\text{ \AA}$ ,  $b=7.121(1)\text{ \AA}$ ,  $c=9.626(3)\text{ \AA}$ , and  $\beta=115.3(1)^\circ$ . There is one crystallographically independent Cs atom, one independent Al atom, one independent B atom and four independent O atoms in the asymmetric unit. The Cs, Al, and B atoms as well as O1, O2 and O4 atoms are at the general positions of Wyckoff sites 4e, while the O3 atom lies on an inversion center of Wyckoff site 2a. The oxidation state of 1+, 3+, 3+ and 2- can be assigned to Cs, Al, B and O atoms, respectively.

The structure of  $\text{Cs}_2\text{Al}_2\text{B}_2\text{O}_7$  is illustrated in Fig. 2. It is a three-dimensional framework built from corner-sharing  $\text{AlO}_4$  tetrahedra and  $\text{BO}_3$  triangles with channels occupied by the  $\text{Cs}^+$  cations. The structure can be considered to be built up from the nearly planar  $[\text{Al}_2\text{B}_2\text{O}_{10}]$  rings, which are composed of two  $\text{AlO}_4$  tetrahedra and two  $\text{BO}_3$  triangles connected alternately to each other by corner-sharing. These rings are further connected by O1 atoms to form layers parallel to  $bc$  plane (Fig. 3). The O3 atom lying at an inversion center and belonging to the  $\text{AlO}_4$  tetrahedra, or in other words, the linear Al–O3–Al, then acts as a linker between layers to generate a three dimensional anionic framework with channels to accommodate the  $\text{Cs}^+$  cations.

Clearly, the alkali metal ( $M$ ) ionic radius has significant effect on the structure of the  $M_2\text{Al}_2\text{B}_2\text{O}_7$  ( $M=\text{Na}$ ,  $\text{K}$ ,  $\text{Rb}$  and  $\text{Cs}$ ) system. They adopt four different structure types. With the increase of the  $M$  ionic radius, the symmetry of the structures descends from space group  $P\bar{3}1c$  ( $\text{Na}_2\text{Al}_2\text{B}_2\text{O}_7$ ) to  $P321$  ( $\text{K}_2\text{Al}_2\text{B}_2\text{O}_7$ ), and then to  $P2_1/c$  ( $\text{Rb}_2\text{Al}_2\text{B}_2\text{O}_7$  and  $\text{Cs}_2\text{Al}_2\text{B}_2\text{O}_7$ ) [10–12]. In  $\text{Na}_2\text{Al}_2\text{B}_2\text{O}_7$ , the  $\text{AlO}_4$  tetrahedra and  $\text{BO}_3$  triangles are connected to form  ${}^2_\infty\text{Al}_2\text{B}_2\text{O}_7^{2-}$  layers parallel to  $ab$  plane, which are separated by  $\text{Na}^+$  cations [11]. In  $\text{K}_2\text{Al}_2\text{B}_2\text{O}_7$ , the  $\text{AlO}_4$  tetrahedra and  $\text{BO}_3$  triangles are also arranged in a layer parallel to the  $ab$  plane, but these layers are further connected by Al–O–Al along the  $c$  direction to build a three-dimensional framework with  $\text{K}^+$  cations located in the channels [10].  $\text{Rb}_2\text{Al}_2\text{B}_2\text{O}_7$  and  $\text{Cs}_2\text{Al}_2\text{B}_2\text{O}_7$

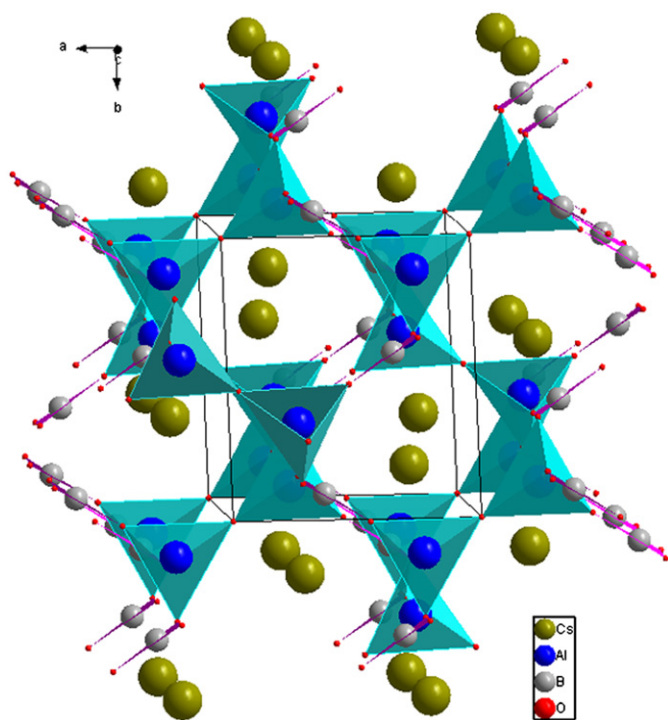


Fig. 2. Crystal structure of  $\text{Cs}_2\text{Al}_2\text{B}_2\text{O}_7$  showing  $\text{AlO}_4$  tetrahedra and  $\text{BO}_3$  triangles viewed down the  $c$  direction.

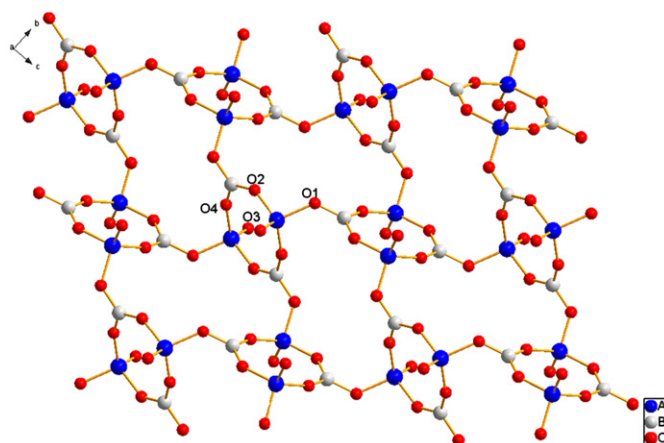


Fig. 3. Structure of the layer composed of the  $[\text{Al}_2\text{B}_2\text{O}_{10}]$  rings in  $\text{Cs}_2\text{Al}_2\text{B}_2\text{O}_7$ .

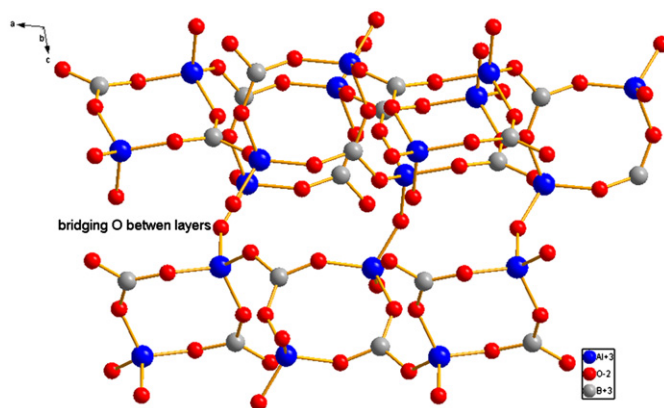


Fig. 4. Connectivity between the  $\text{AlO}_4$  and  $\text{BO}_3$  polyhedra in  $\text{Rb}_2\text{Al}_2\text{B}_2\text{O}_7$ .

crystallize in the same space group  $P2_1/c$  and adopts similar three-dimensional framework built from  $\text{AlO}_4$  tetrahedra and  $\text{BO}_3$  triangles. Their subtle structural difference lies in two aspects: First, the unit cell of  $\text{Rb}_2\text{Al}_2\text{B}_2\text{O}_7$  ( $a=8.901(2)\text{ \AA}$ ,  $b=7.539(1)\text{ \AA}$ ,  $c=11.905(2)\text{ \AA}$ ,  $\beta=103.97(1)^\circ$ ,  $V=775.3(2)\text{ \AA}^3$ ) can be considered twice as large as that of  $\text{Cs}_2\text{Al}_2\text{B}_2\text{O}_7$  and thus the asymmetric unit of  $\text{Rb}_2\text{Al}_2\text{B}_2\text{O}_7$  structure contains two crystallographically unique Rb, two Al, two B and seven O atoms, all at general positions. Second, although in the structure of  $\text{Rb}_2\text{Al}_2\text{B}_2\text{O}_7$ , the  $[\text{Al}_2\text{B}_2\text{O}_{10}]$  rings also form layers parallel to the  $ab$  plane, but the bridging O atom between these layers are located at a general position and the bond angle of the bridging Al–O–Al is  $146.9(2)^\circ$  (Fig. 4), while the bridging O atom between these layers in  $\text{Cs}_2\text{Al}_2\text{B}_2\text{O}_7$  lies on an inversion center with the bridging Al–O–Al bond angle of  $180^\circ$ .

In all these four compounds, only  $\text{K}_2\text{Al}_2\text{B}_2\text{O}_7$  crystallizes in a non-centrosymmetric space group with the two sets of  $\text{BO}_3$  groups, the major nonlinear optical active units, twisting about  $37^\circ$ , which gives it moderate second harmonic generation (SHG) response. In the Na, Rb, and Cs analogs, the  $\text{BO}_3$  groups are related to each other through an inversion center, so none of them has SHG effect.

The bond distances and angles in  $\text{Cs}_2\text{Al}_2\text{B}_2\text{O}_7$  are normal. The  $\text{AlO}_4$  is a slightly distorted tetrahedron with the Al–O bond distances ranging from  $1.708(1)\text{ \AA}$  to  $1.749(3)\text{ \AA}$  and the O–Al–O angles ranging from  $103.5(1)^\circ$  to  $114.5(1)^\circ$ . In the  $\text{BO}_3$  triangles, the lengths of B–O bonds range from  $1.353(4)$  to  $1.375(4)\text{ \AA}$  and the O–B–O angle lie between  $118.7(3)^\circ$  and  $122.2(3)^\circ$ . These bond distances and angles compare well with the related  $M_2\text{Al}_2\text{B}_2\text{O}_7$

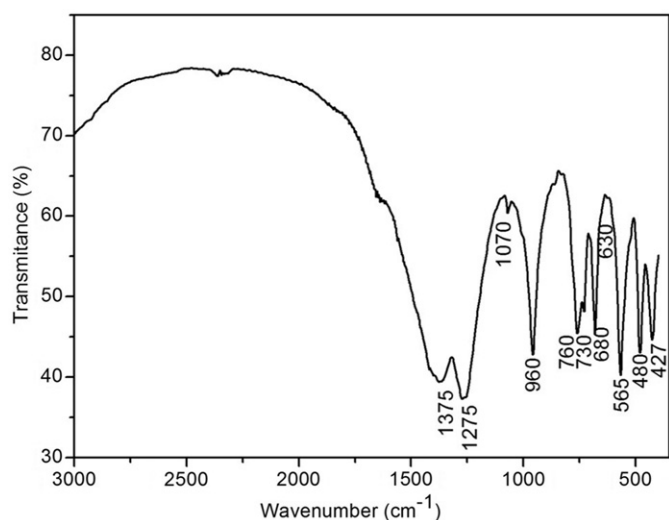


Fig. 5. Infrared spectrum of  $\text{Cs}_2\text{Al}_2\text{B}_2\text{O}_7$ .

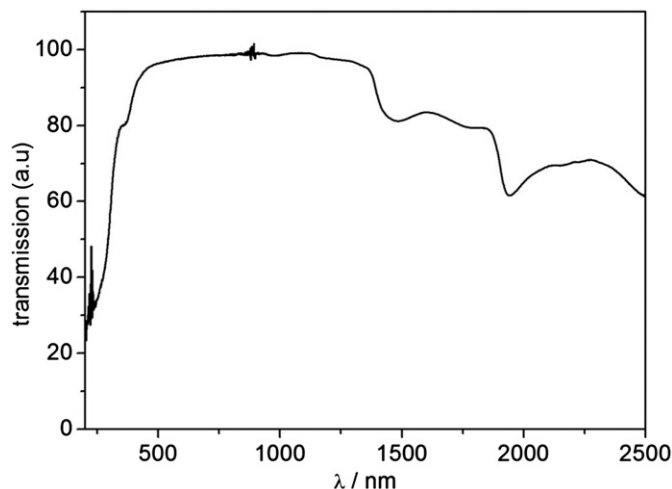


Fig. 6. Diffuse reflectance spectrum of  $\text{Cs}_2\text{Al}_2\text{B}_2\text{O}_7$ .

( $M=\text{Na, K, Rb}$ ) structures [10–12]. As for the  $\text{Cs}^+$  cation, the distances of  $\text{Cs}-\text{O}$  in  $\text{Cs}_2\text{Al}_2\text{B}_2\text{O}_7$  range from 3.070(3) to 3.600(3) Å, which resemble those in  $\text{CsB}_3\text{O}_5$  (3.030(3) Å to 3.342(6) Å) and  $\text{CsLiB}_6\text{O}_{10}$  (3.147(3) Å to 3.342(6) Å) [3,16].

### 3.3. Infrared spectroscopy

In order to confirm the coordination surroundings of B and Al atoms in the  $\text{Cs}_2\text{Al}_2\text{B}_2\text{O}_7$  structure, infrared spectrum measurement was carried out and the spectrum from 400 to 3000  $\text{cm}^{-1}$  is shown in Fig. 5. The peaks at 1374, 1274, 1070, 730, 680, 629, and 565  $\text{cm}^{-1}$  can be attributed to asymmetric stretching and symmetric stretching vibrations of  $\text{BO}_3$  groups [17–22] and those at

960, 760, 480, and 427  $\text{cm}^{-1}$  are likely to be the asymmetric and symmetric stretching of  $\text{Al}-\text{O}$  in  $\text{AlO}_4$  [18,23,24], respectively.

### 3.4. UV–vis–NIR diffuse reflectance spectrum

The UV–vis–NIR diffuse reflectance spectrum of  $\text{Cs}_2\text{Al}_2\text{B}_2\text{O}_7$  in the region of 200–2500 nm is shown in Fig. 6. It is clear that  $\text{Cs}_2\text{Al}_2\text{B}_2\text{O}_7$  has obvious absorption below 300 nm and the optical band gap of  $\text{Cs}_2\text{Al}_2\text{B}_2\text{O}_7$  can be estimated to be 4.13(2) eV by the straightforward extrapolation method [25].

### Acknowledgments

This research was supported by the National Basic Research Project of China (No. 2010CB630701) and National Natural Science Foundation of China (No. 51072203).

### Appendix A. Supplementary materials

Supplementary data associated with this article can be found in the online version at doi:10.1016/j.jssc.2011.10.023.

### References

- [1] C.T. Chen, B. Wu, A. Jiang, G. You, *Sci. Sin. B* 28 (1985) 235–243.
- [2] C.T. Chen, Y. Wu, A. Jiang, B. Wu, G. You, R. Li, S. Lin, *J. Opt. Soc. Am. B* (1989) 616–621.
- [3] J.M. Tu, D.A. Keszler, *Mater. Res. Bull.* 30 (1995) 209–215.
- [4] B.C. Wu, D.Y. Tang, N. Ye, C.T. Chen, *Opt. Mater.* 5 (1996) 105–109.
- [5] F. Kong, S.P. Huang, Z.M. Sun, J.G. Mao, W.D. Cheng, *J. Am. Chem. Soc.* 128 (2006) 7750–7751.
- [6] A. Haberer, R. Kaindl, O. Oeckler, H. Huppertz, *J. Solid State Chem.* 183 (2010) 1970–1979.
- [7] S.C. Wang, N. Ye, W. Li, D. Zhao, *J. Am. Chem. Soc.* 132 (2010) 8779–8786.
- [8] Y.G. Wang, R.K. Li, *J. Solid State Chem.* 183 (2010) 1221–1225.
- [9] H.W. Yu, S.L. Pan, H.P. Wu, J. Han, X.Y. Dong, Z.X. Zhou, *J. Solid State Chem.* 184 (2011) 1644–1648.
- [10] Z.G. Hu, T. Higashiyama, M. Yoshimura, Y. Mori, T. Sasaki, *Z. Kristallogr.—New Cryst. Struct.* 214 (1999) 433–434.
- [11] M. He, X.L. Chen, T. Zhou, B.Q. Hu, Y.P. Xu, T. Xu, *J. Alloys Compd.* 327 (2001) 210–214.
- [12] J.L. Kissick, D.A. Keszler, *Acta Crystallogr. Sect. E: Struct. Rep. Online* 58 (2002) 185–187.
- [13] Rigaku, CrystalClear, Rigaku Corporation, Tokyo, Japan, 2008.
- [14] G.M. Sheldrick, *Acta Crystallogr. A* 64 (2008) 112–122.
- [15] L.M. Gelato, E. Parthe, *J. Appl. Crystallogr.* 20 (1987) 139–143.
- [16] J. Krogh-Moe, *Acta Crystallogr. Sect. B: Struct. Sci.* 30 (1974) 1178–1180.
- [17] L.F. Zhou, H.X. Lin, W. Chen, L. Luo, *J. Phys. Chem. Solids* 69 (2008) 2499–2502.
- [18] Y. Cheng, H.N. Xiao, S.G. Chen, B.Z. Tang, *Physica B* 404 (2009) 1230–1234.
- [19] V. Jubera, J. Sablayrolles, F. Guillen, R. Decourt, M. Couzi, A. Garcia, *Opt. Commun.* 282 (2009) 53–59.
- [20] M.I. Pashchenko, V.A. Bedarev, V.I. Kut'ko, L.N. Besmaternykh, V.L. Temerov, *Low Temp. Phys.* 36 (2010) 638–641.
- [21] T. Sun, H.N. Xiao, W.M. Guo, X.C. Hong, *Ceram. Int.* 36 (2010) 821–826.
- [22] J.J. Li, S.L. Pan, W.W. Zhao, X.L. Tian, J. Han, X.Y. Fan, *J. Mol. Struct.* 994 (2011) 321–324.
- [23] J.H. Park, D.J. Min, H.S. Song, *ISIJ Int.* 42 (2002) 38–43.
- [24] A. Nag, T.R.N. Kutty, *Mater. Res. Bull.* 39 (2004) 331–342.
- [25] O. Schevciw, W.B. White, *Mater. Res. Bull.* 18 (1983) 1059–1068.